UMYU Scientifica, Vol. 5 NO. 1, March 2026, Pp 133 – 142
https://doi.org/10.56919/usci.2651.012
ISSN: 2955 – 1145 (print); 2955 – 1153 (online)
A periodical of the Faculty of Natural and Applied Sciences, UMYU, Katsina

ORIGINAL RESEARCH ARTICLE

Chemical Surface Functionalization of Woven Kenaf Preforms Using Methyl Methacrylate and Methyl Acrylate Monomers

Mohammed J. Bello[1&2], Jamila B. Ali[1], Abdullahi Danladi[1], Muktari Suleiman[1] and Hussaini D. Ibrahim[2]
[1]Department of Polymer and Textile Engineering, Faculty of Engineering, Ahmadu Bello University, Zaria, Nigeria
[2]Raw Materials Research and Development Council, Maitama, Abuja, Nigeria

ABSTRACT
This study investigated the surface modification of woven kenaf preforms to overcome their inherent hydrophilicity and enhance their thermal and surface properties. Graft copolymerization was carried out using methyl methacrylate (MMA) and methyl acrylate (MA) through a Fenton's reagent-initiated free radical process under a nitrogen atmosphere. Fourier Transform Infrared (FTIR) analysis confirmed the formation of ester linkages, evidenced by characteristic carbonyl absorption peaks at 1725 cm^{-1}. The grafting percentage and efficiency were 22% and 46.2% for MMA, and 21.7% and 45.1% for MA, respectively, indicating effective monomer incorporation onto the kenaf preform surface. Thermogravimetric analysis (TGA) revealed enhanced thermal stability, with onset degradation temperatures increasing from 233.3°C for ungrafted kenaf to 275°C and 292°C for MMA- and MA-grafted samples, respectively. Similarly, the maximum degradation temperature increased from 275°C to 370°C and 365°C for MMA- and MA-grafted samples, respectively. Scanning Electron Microscopy (SEM) analysis revealed increased surface roughness and a uniform polymer coating on the modified preform, indicating successful coverage. These findings demonstrate that graft copolymerization significantly improves the thermal stability and surface characteristics of woven kenaf preforms.

ARTICLE HISTORY
Received January 03, 2026
Accepted March 10, 2026
Published March 15, 2026

KEYWORDS
2D Weaving, Graft copolymerization, kenaf preform, and Thermal stability

INTRODUCTION
Surface modification of natural fibers via graft copolymerization has emerged as an effective approach to improve their compatibility with polymer matrices (Xie et al., 2010; Kabir et al., 2012). Methyl methacrylate (MMA) and methyl acrylate (MA) are widely utilized monomers in this context due to their high reactivity and ability to form durable covalent bonds with cellulose-based materials (Kalia et al., 2011; Thakur & Thakur, 2014). Grafting these monomers onto natural fibers enhances mechanical strength, thermal stability, and moisture resistance, while reducing their inherent hydrophilicity (Bledzki & Gassan, 1999; John & Thomas, 2008).

Kenaf (*Hibiscus cannabinus*) is a bast fiber characterized by low density, high specific strength, biodegradability, and a high cellulose content, making it an attractive and sustainable reinforcement material (Akil et al., 2011; Faruk et al., 2012). It has been widely explored for applications in automotive, construction, packaging, and acoustic materials (Pickering et al., 2016; Jawaid & Abdul Khalil, 2011). Kenaf-based systems have demonstrated promising mechanical performance and environmental advantages compared to conventional glass fiber materials (Tomaz, 2021; Faruk et al., 2012; Pickering et al., 2016).

Natural fibers have gained considerable attention as sustainable reinforcements in polymer composites due to their renewability, biodegradability, and favorable mechanical properties. Jute fiber, for instance, has been shown to significantly enhance the tensile and flexural properties of polypropylene composites, with fiber–matrix interactions playing a critical role in determining overall performance (Danladi et al., 2025). Similarly, lignocellulosic fillers derived from agricultural waste, such as *Prosopis africana* pods, have been successfully utilized in epoxy-based composites for interior cladding applications, demonstrating that bio-derived materials can serve as viable alternatives to conventional synthetic reinforcements (Jibril et al., 2025). Furthermore, the incorporation of ground rubber tire filler into recycled high-density polyethylene has revealed that filler particle size substantially influences morphological homogeneity and mechanical performance, underscoring the importance of filler characteristics in composite design

Correspondence: Mohammed J. Bello. Department of Polymer and Textile Engineering, Faculty of Engineering, Ahmadu Bello University, Zaria, Nigeria. ✉ mobellojiyah1920@gmail.com.
How to cite: Bello, M. J., Ali, J. B., Danladi, A., Suleiman, M., & Ibrahim, H. D. (2026). Chemical Surface Functionalization of Woven Kenaf Preforms Using Methyl Methacrylate and Methyl Acrylate Monomers. *UMYU Scientifica*, 5(1), 133 – 142. https://doi.org/10.56919/usci.2651.012

(Abdulkadir et al., 2025). These studies collectively highlight the growing potential of waste-derived and natural fillers in developing sustainable composite materials.

Despite these advantages, the inherent hydrophilicity of kenaf remains a significant limitation, particularly in its woven preform architecture (Kabir et al., 2012; Xie et al., 2010). Existing studies have largely focused on modifying natural fibers in their individual, random, or particulate forms, with limited attention to structured fiber assemblies, such as woven preforms (Jawaid & Abdul Khalil, 2011; Pickering et al., 2016). This study therefore, investigates the surface modification of woven kenaf preforms via graft copolymerization with MMA and MA, aiming to improve surface characteristics and reduce hydrophilicity.

MATERIALS AND METHODS

Kenaf yarn was purchased from Juntextile, China. Methyl methacrylate ($C_5H_8O_2$), Methyl acrylate ($C_4H_6O_2$) and analytical grade hydrogen peroxide (H_2O_2), sodium hydroxide (NaOH) were purchased from Bristol chemicals, Acetone $(CH_3)_2CO$ and ferrous ammonium salt ($FeSO_4(NH_2)_2SO_4.6H_2O$), were purchased from sigma Aldrich and Nitrogen gas (N_2), 2000 mL 3-neck round bottom flask, 2000 mL beaker and pH meter from Raw Materials Research and Development Council Laboratory at African University of Science and Technology was used to carry out the grafting experiment. AD-A-HARNESS (L.W. MACOMBER) floor loom, model B4D, serial number 1409, ABU Zaria, Nigeria, was used to weave kenaf yarn into a preform.

Removal of the inhibitor from the MMA monomer

Methyl methacrylate (MMA) and methyl acrylate (MA) were purified to remove their inhibitors (hydroquinone) by passing them through a column packed with activated alumina. The purification setup consisted of a burette fitted with glass wool and activated alumina, mounted on a retort stand, while the reagent bottles were immersed in an ice bath to maintain a low temperature. As MMA and MA were passed through the column in separate experiments, the activated alumina changed color from white to pink, indicating the adsorption of the inhibitor. The purified MMA and MA were collected in reagent bottles and stored at 10 °C or below in the laboratory refrigerator for subsequent use.

2D weaving of kenaf Yarn into a preform

Kenaf yarn was woven on an AD-A-HARNESS (L.W. MACOMBER) floor loom, model B4D, serial number 1409. This is a traditional, sturdy loom setup with a four-shaft model shuttle and reed system that requires manual warp and weft insertions. Plain weave was the design of choice for this research because of its simplicity and its tight, uniform structure, which is ideal for creating a balanced preform that can be impregnated with infusion resin for composite preparation. Each of the repeat patterns took 35 minutes to complete, a timeframe shaped by the need to maintain a consistent beating force between 4 and 5 on a subjective effort scale, where 1 was a light tap, and 10 was a too-heavy slam for the weaving process. Figure 1 and 2 show the weaving and a woven kenaf preform respectively.

Figure 1: Weaving kenaf preform using a floor loom

Figure 2: Woven kenaf preform

Grafting process

The method and procedure described by Kalia et al. (2009) and Thakur et al. (2014) were adopted for grafting. A 2000 mL 3-neck round-bottom flask was used for the grafting process. The flask was purged for 15 minutes with nitrogen gas at a pressure of 0.1–0.2 bar, with the flow rate maintained at 50–100 mL/min. The 3-neck 2000 mL round-bottom flask, fixed and coupled with a reflux condenser, a glass stirring rod, and a retort stand, was adjusted to sit firmly on a water bath. Sodium hydroxide (NaOH)- treated kenaf (9.88 g) was introduced into a 2000 mL 3-neck round-bottom flask with a tong. Fenton's solution was added to the reaction medium, and nitrogen gas was activated to purge any available oxygen in the combined mixture of pretreated kenaf preform and Fenton's reagent for 10 minutes. 5 mL Methyl methacrylate monomer was slowly added to the reaction medium, which was stirred with a glass rod to ensure an even mixture with Fenton's reagent and preform. The water bath temperature was maintained at 50 °C for 1 hour and 30 minutes. The grafted kenaf product was further treated by removing the PMMA homopolymer formed during the reaction. The grafting reaction was carried out using a Fenton's reagent system, with ferrous ion concentration [Fe^{2+}] of 6.8 mM (0.0068 M) and hydrogen peroxide concentration [H_2O_2] of 0.235 M (235 mM), corresponding to a molar ratio of Fe^{2+} to H_2O_2 of 1:35. The monomer to preform ratio was maintained at 0.5:1

during the graft copolymerization process. All grafting experiments were conducted in triplicate (n = 3), and the average values were reported.

Stoichiometry of the reaction

The graft copolymerization was initiated by Fenton's reagent (Fe^{2+}/H_2O_2), which generates highly reactive hydroxyl radicals (•OH) capable of abstracting hydrogen atoms from the kenaf preform (cellulose backbone) to create macro-radical sites. The reaction pH was 2.9

Primary reaction: $Fe^{2+} + H_2O_2 \rightarrow Fe^{3+} + •OH + OH^-$

In the presence of excess H_2O_2, the ferric ion (Fe^{3+}) is partially reduced back to ferrous ion (Fe^{2+}), allowing a limited catalytic cycle: $Fe^{3+} + H_2O_2 \rightarrow Fe^{2+} + HO_2• + H^+$ (where $HO_2•$ is the hydroperoxyl radical, less reactive than •OH). Hydroxyl radical (•OH) is the main oxidant responsible for initiating grafting by abstracting a hydrogen atom from the cellulose chain:

Kenaf–H + •OH → Kenaf• + H_2O

Generation of hydroxyl radicals (Fenton's reaction)

a. $Fe^{2+} + H_2O_2 \rightarrow Fe^{3+} + •OH + OH^-$

b. Formation of cellulose macro-radicals (Hydrogen abstraction)

Cellulose–H + •OH → Cellulose• + H_2O

c. Initiation of grafting (Addition of MMA to cellulose radical)

Cellulose• + $CH_2=C(CH_3)COOCH_3$ → Cellulose–CH_2–C•$(CH_3)COOCH_3$

d. Propagation (Growth of PMMA side chains)

Cellulose–CH_2–C•$(CH_3)COOCH_3$ + n $CH_2=C(CH_3)COOCH_3$ → Cellulose–$[CH_2–C(CH_3)(COOCH_3)]_n$–$CH_2$–C•$(CH_3)COOCH_3$

e. Termination

Combination: Cellulose $[CH_2–C(CH_3)(COOCH_3)]_n$–$CH_2$–C•$(CH_3)COOCH_3$ + •R → Cellulose–g-PMMA (where •R is another radical, another growing chain)

Generation of hydroxyl radicals involving MA and Fenton reaction:

a. Fenton Radical Generation

$Fe^{2+} + H_2O_2 \rightarrow Fe^{3+} + •OH + OH^-$

b. Hydrogen Abstraction

Kenaf–H + •OH → Kenaf• + H_2O

c. Initiation

Kenaf• + $CH_2=CHCOOCH_3$ → Kenaf–CH_2–CH•$(COOCH_3)$

d. Propagation

Kenaf–CH_2–CH•$(COOCH_3)$ + n$CH_2=CHCOOCH_3$ → Kenaf–$[CH_2–CH(COOCH_3)]_n$–CH_2–CH•$(COOCH_3)$

e. Termination by Combination

Kenaf–$[CH_2–CH(COOCH_3)]_n$–CH_2–CH•$(COOCH_3)$→Kenaf–$[CH_2–CH(COOCH_3)]_n$–$CH(COOCH_3)$–$CH(COOCH_3)$–$[CH_2–CH(COOCH_3)]_n$–Kenaf

Removal of homopolymer and determination of graft level

After completion of the graft copolymerization reaction, the kenaf preforms were separated from the reaction mixture and subjected to thorough removal of poly (methyl methacrylate) (PMMA) and (PMA) homopolymer, unreacted monomer, and residual Fenton's reagent (Fe^{2+}/Fe^{3+} and H_2O_2). The preforms were first rinsed repeatedly with distilled water to remove water-soluble residues. Subsequently, the homopolymer was removed by solvent extraction using acetone. The extraction procedure was as follows: Each preform was immersed in 50 mL of fresh acetone and agitated (using a mechanical shaker at 150 rpm) for 30 minutes at room temperature. This is followed by washing repeatedly three times with fresh 50 mL portions of acetone at each interval to ensure complete removal of the homopolymer. After the final acetone wash, the preforms were rinsed once with distilled water to remove any residual acetone, then air-dried at room temperature (25 ± 2 °C) for 24 hours. The preforms were subsequently dried at 60 °C to

constant weight until no further weight loss was observed. The completeness of homopolymer removal was confirmed by the absence of further weight loss in an additional acetone wash of the final acetone extract. The weight of the dried grafted kenaf preform (free of homopolymer) was then recorded. The grafting percentage (% G) and grafting efficiency (% E) were calculated using the following equations:

$$\%G = [(W_1 - W_0) / W_0] \times 100 \quad \ldots\ldots\ldots\ldots\ldots\ldots\ldots\ldots\ 1$$

$$\%E = [(W_1 - W_0) / (W_1 - W_0 + W_2)] \times 100 \quad \ldots\ldots\ldots\ldots 2$$

Equation 2 is adopted from Abu Bakar *et al.,* (2008) .

Where:

W_0 = initial dry weight of ungrafted kenaf preform (g)
W_1 = dry weight of grafted kenaf preform after homopolymer removal (g)
W_2 = weight of extracted PMMA homopolymer (determined by evaporation of combined acetone extracts to constant weight, where applicable)

Fourier transform infrared spectroscopy

FTIR spectra of kenaf preform, PMMA, kenaf-*g*-PMMA, and PMA were recorded on a Fourier transform IR spectrometer (Pelkin Elmer Spectrum 2000) using a KBr disk pellet to identify the functional groups present in the kenaf preform, PMMA, PMA, kenaf-*g*-PMMA, and kenaf-g-PMA

3.1 Thermo-gravimetric analysis

Thermo-gravimetric experiments were carried out using a Perkin-Elmer thermal analyzer. This analysis was carried out in a nitrogen atmosphere from 35 °C to 1000 °C at a heating rate of 10 °Cmin^{-1} with a nitrogen flow rate of 50 ml min^{-1}. Thermo-grams were obtained by plotting percentage residual weight against temperature. This study is used to identify the degradation temperature of kenaf preform, kenaf-*g*-PMMA, and kenaf-g-PMA

Scanning electron microscopy

Scanning electron microscopy was used to study the surface morphologies of grafted and raw kenaf preforms (Phenom Pro X, Model 800-07334). The samples were mounted on the stub and sputter-coated with a thin layer of gold to avoid electrostatic charging during examination.

RESULTS AND DISCUSSION

Free radical graft copolymerization reaction analysis

Parameters of the grafting reaction used to produce kenaf-g-PMMA and kenaf-g-PMA were obtained from similar research by Abdul Aziz et al. (2014), who synthesized chitosan-grafted-poly(methyl methacrylate) using Fenton's reagent with some modifications to the grafting method. The grafting method used was based on the research by Kalia et al. (2009) and Thakur et al. (2014). In this study, the grafting percentage and grafting efficiency were 22 % for MMA, 21.7 % for MA, 46.7 % for MMA, and 45.1 % for MA, respectively. Based on a previous study by Abdul Aziz *et al.* (2014) and with modifications in this research work, grafting was carried out at 50 °C for 120 minutes under Nitrogen and a pH of 2.9. Grafting percentage and efficiency results indicated that MMA and MA monomers were successfully grafted onto the kenaf preform surface.

Fourier transform infrared spectroscopy

Table 1: FTIR Table for Grafted and Ungrafted Kenaf preforms

Wavenumber (cm^{-1})	Functional Group Assignment	Ungrafted Kenaf	MA-Grafted Kenaf	MMA-Grafted Kenaf
3214	O–H stretching vibration	Present	Present	Present
2922	C–H stretching vibration (aliphatic)	Present	Present	Present
1725	C=O stretching vibration (ester carbonyl)	Absent	Present	Present
1466	CH_2 bending vibration	Present	Present	Present
1373	C–H / O–H in-plane bending	Present	Present	Present
1319	C–O stretching / CH_2 wagging	Present	Present	Present
1249	C–O stretching	Present	Present	Present
1160	C–O–C asymmetric stretching (glycosidic)	Present	Present	Present
1056	C–O stretching (cellulose/hemicellulose)	Present	Present	Present

Table 2: Thermal degradation temperatures (T_{onset} and T_{max}) of ungrafted and grafted kenaf preforms

Sample	Tonset (°C)	Tmax (°C)
Ungrafted kenaf	233.3 ± 3.5	275.0 ± 5.0
Grafted kenaf (MMA)	287.7 ± 6.8	365.0 ± 5.0
Grafted kenaf (MA)	292.0 ± 6.1	365.0 ± 5.0

FTIR spectra of ungrafted kenaf fibers obtained from woven preforms revealed the characteristic constituents of lignocellulosic materials, including cellulose, hemicellulose, lignin, pectin, and traces of waxes (Figure 3). Broad absorption bands at 3400–3300 cm^{-1} correspond to O–H stretching vibrations of hydroxyl groups in cellulose and hemicellulose, indicating the hydrophilic nature of the fibers (Table 1). The peak at

2900 cm^{-1} represents C–H stretching of aliphatic groups, while the C–O stretching in glycosidic linkages of cellulose appeared at 1050–1030 cm^{-1}. The carbonyl (C=O) stretching vibration around 1730–1740 cm^{-1} is attributed to acetyl and ester groups in hemicellulose (Jonoobi et al., 2011; Tserki et al., 2005). Lignin-related peaks were observed at 1600–1500 cm^{-1} (aromatic C=O) and 1240–1260 cm^{-1} (C–O of syringic units), consistent with earlier reports (Khalil et al., 2010). Minor peaks at 720 cm^{-1} were associated with long-chain hydrocarbons from waxes. For kenaf grafted with MMA, a pronounced carbonyl peak at 1725 cm^{-1} confirmed successful grafting, with reduced transmittance within 2800–3000 cm^{-1} (notably at 2894 cm^{-1}) reflecting incorporation of methyl groups. A slight shift in the C–O stretching region near 1236 cm^{-1} indicated ester linkage formation, consistent with the incorporation of MMA on the fiber backbone (Tee et al., 2013; Abdul Aziz et al., 2014). Similarly, kenaf grafted with MA exhibited a strong carbonyl absorption near 1725 cm^{-1} and a C–H stretching band at 2894 cm^{-1}, characteristic of MA grafting, which has a simpler vinyl structure lacking the methyl group present in MMA (Athawale et al., 2000).

Thermogravimetric Analysis

Thermogravimetric analysis (TGA) was performed in triplicate (n = 3) for each sample to ensure reproducibility. The thermos-gravimetric (TGA) profile of ungrafted kenaf preform showed a typical multi-stage decomposition pattern characteristic of lignocellulosic fibers composed of cellulose, hemicellulose, and lignin. A gradual weight loss below 200 °C corresponded to moisture evaporation and volatile release (Yang et al., 2007). Major degradation occurred between 200–400 °C (Table 2), attributed to the decomposition of hemicellulose (200–260 °C) and cellulose (300–350 °C), as similarly reported by Poletto et al. (2012) where they examined how wood composition and cellulose crystallite size affect thermal decomposition in four wood species using thermos-gravimetric they found that species with higher extractive content **and** smaller, less crystalline cellulose decompose faster and have lower thermal stability.

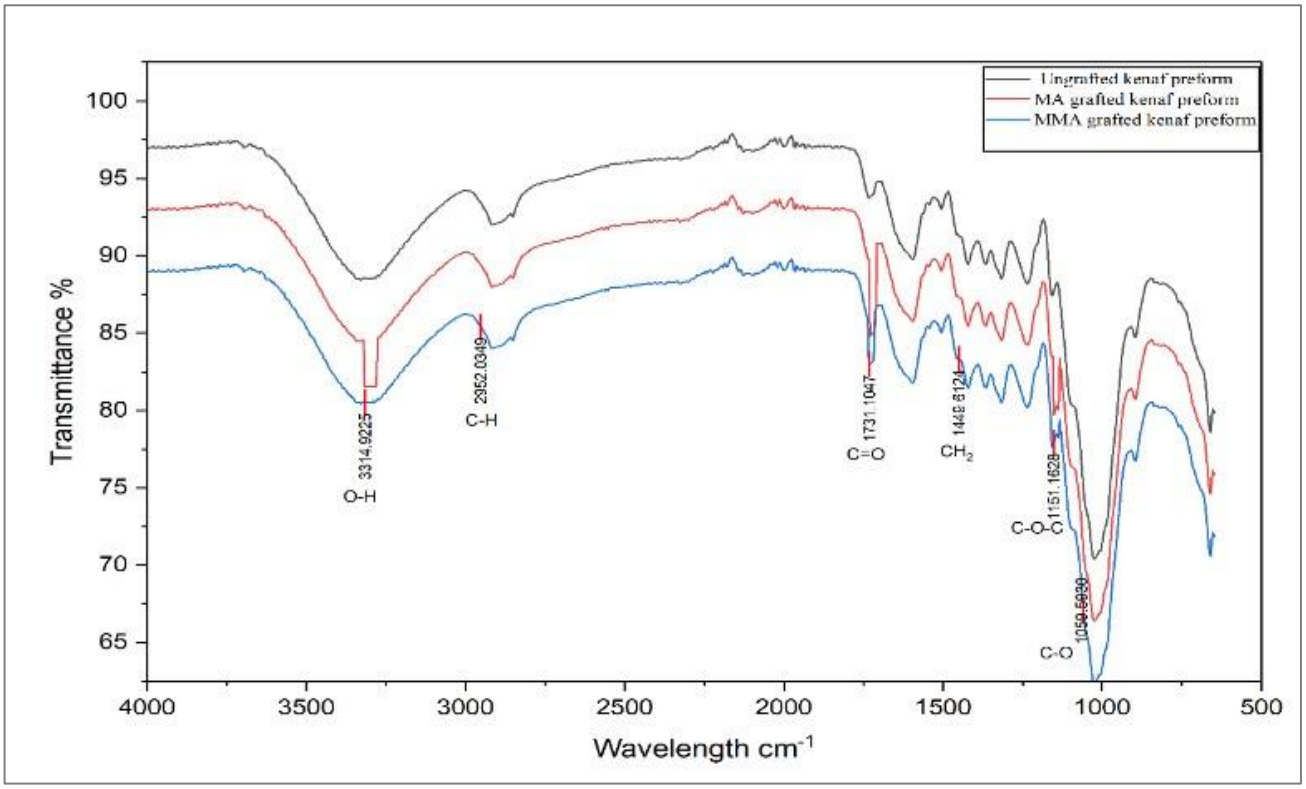

Figure 3: FTIR spectra of Ungrafted kenaf, grafted kenaf with MMA, and grafted kenaf with MA

Beyond 400 °C, lignin degradation became dominant, extending to 800 °C due to its higher thermal stability (Yang et al., 2006). The residual char of 15–20% at 800 °C was consistent with the formation of inorganic ash, confirming findings by Sanchez-Silva et al. (2012). Their results yielded DTG curves that showed distinct peaks whose temperatures increased with higher heating rates, suggesting heat-transfer limitations within cellulose particles.

Kenaf preform grafted with methyl methacrylate (MMA) exhibited enhanced thermal stability. The initial weight loss below 120 °C was attributed to moisture removal, as observed for other natural fibers (George et al., 2016). Primary decomposition occurred between 300–450 °C, with a DTG peak near 400 °C, higher than the ungrafted preform (270–275 °C), indicating improved thermal resistance due to grafted MMA chains (Mwaikambo & Ansell, 2002). The 10 % residue at 800 °C confirmed increased char yield and cross-linking, consistent with enhanced fiber stability (Sanjay et al., 2018).

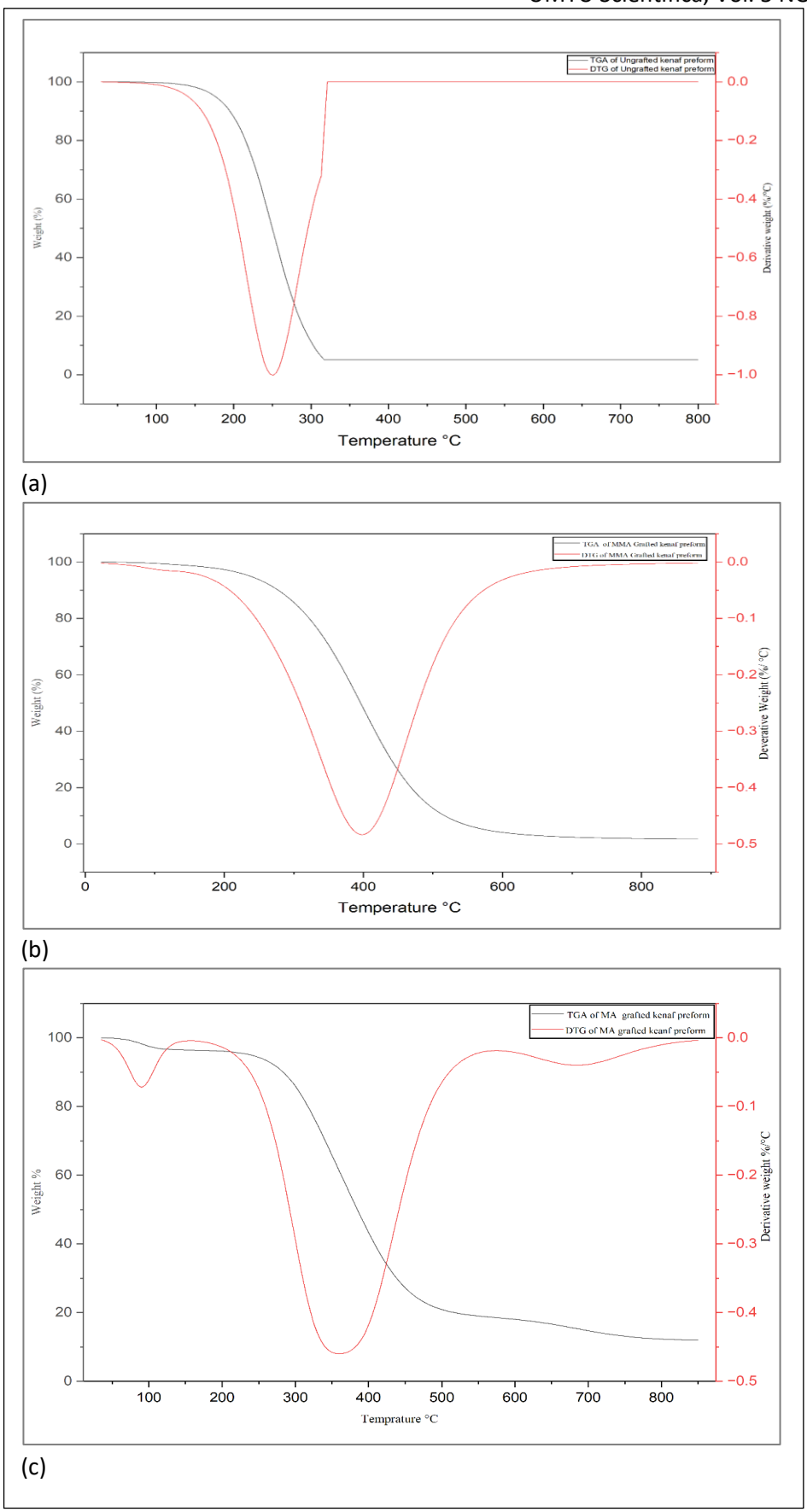

Figure 4: TGA/DTG profiles of (a) Ungrafted kenaf, (b) Grafted kenaf with MMA, (c) Grafted kenaf with MA

Similarly, kenaf grafted with methyl acrylate (MA) displayed a comparable thermal profile. The first weight loss below 150 °C corresponded to moisture loss (John & Thomas, 2008). Primary degradation occurred at 270–430 °C, with a DTG peak at 360–370 °C, higher than that of the raw fiber but slightly lower than that of the MMA-grafted samples. This can be attributed to the shorter chain length and lower cross-linking density of MA (Sinha

& Rout, 2008; Gupta et al., 2013). Nonetheless, MA grafting improved thermal endurance by reducing hygroscopicity and introducing hydrophobic polymeric segments (Li et al., 2007). Figure 4 shows TGA/DTG profiles of ungrafted kenaf, grafted kenaf with MMA, and grafted kenaf with MA.

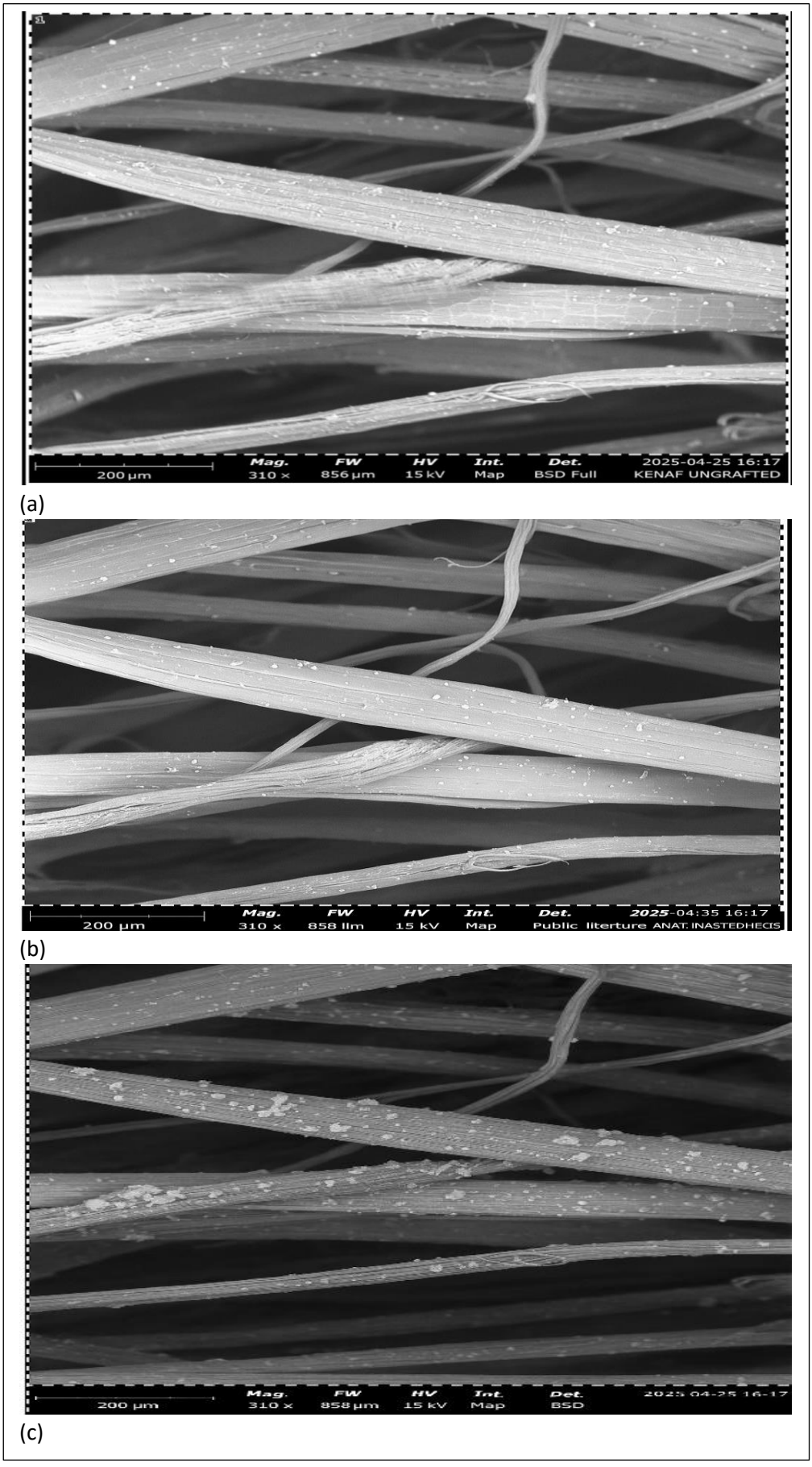

Figure 5: SEM micrographs of (a) Ungrafted kenaf (b) Grafted kenaf with MMA (c) Grafted kenaf with MA

Scanning Electron Microscopy

The SEM micrograph of the ungrafted kenaf preform showed a relatively smooth fiber surface with minor irregularities and loose particles (Figure 5). The limited surface roughness suggests minimal mechanical interlocking between the fiber and the resin. This morphology is characteristic of untreated lignocellulosic fibers, which contain hemicellulose and lignin and contribute to their hydrophilic nature and poor compatibility with hydrophobic polymer matrices. Similar weak fiber-matrix bonding and fiber pull-out were reported for untreated kenaf fibers in a PLA matrix (Huda et al., 2006). In contrast, the SEM micrograph of the kenaf preform grafted with methyl methacrylate (MMA) showed a roughened, polymer-coated surface, indicating successful grafting and surface modification. The presence of polymer granules and the enhanced surface texture promote better resin impregnation and mechanical interlocking, as also observed in acrylate-grafted natural fibers (Panthapulakkal & Sain, 2007). This enhanced adhesion suggests improved interfacial bonding and load transfer capability within the composite. Similarly, kenaf preforms grafted with methyl acrylate (MA) exhibited a more uniformly coated surface with improved wetting characteristics. The SEM image indicated higher polymer deposition and stronger preform fiber-matrix interactions, despite slightly lower grafting efficiency than with MMA. This uniform coating reflects enhanced surface compatibility, resulting in better adhesion and structural integration within the kenaf preform.

CONCLUSION

Graft copolymerization of woven kenaf preforms with methyl methacrylate (MMA) and methyl acrylate (MA) using Fenton's reagent was successfully carried out. FTIR analysis confirmed the formation of ester linkages between the monomers and the kenaf preform surface. Thermogravimetric analysis demonstrated significant improvement in thermal stability, while scanning electron microscopy revealed enhanced surface roughness and polymer coating. These modifications reduced the kenaf preform's inherent hydrophilicity and improved its compatibility with hydrophobic polymer matrices. The grafted woven kenaf shows strong potential as an eco-friendly reinforcement for thermally stable polymer composites, particularly in automotive, construction, and packaging applications in Nigeria. Further studies on the mechanical properties of the resulting composites and on the optimization of grafting parameters are recommended.

FUNDING STATEMENT

This research was self-funded by the corresponding author.

AUTHORS' CONTRIBUTION

The authors confirm their contributions to the paper as follows: Mohammed Jiyah Bello contributed to the design of the experiment and sourcing of kenaf yarn and chemical reagents, and carried out the surface modification of the woven kenaf preform. **Jamila Baba-Ali** reviewed the results. **Abdullahi Danladi** reviewed the results and approved the manuscript for submission. **Hussaini Doko Ibrahim** contributed to the selection, design, and weaving of kenaf yarn into a preform. **Mukhtari Suleiman** evaluated the grafting process and analyzed all characterization results. All authors reviewed the results and approved the final version of the manuscript.

CONFLICT OF INTEREST

We declare that there is no conflict of interest regarding this research study.

REFERENCES

Abdul Aziz, N. A., Abu Bakar, A., Hassan, A., & Azmi, N. (2014). Synthesis of chitosan-grafted poly(methyl methacrylate) using Fenton's reagent as a redox initiator. *Malaysian Journal of Analytical Sciences, 18*(2), 415–422.

Abdul Aziz, S., Tee, T. T., Sanyang, M. L., Rahman, N. A., Hazwan, C. M., & Abdullah, Z. (2014). Grafting of methyl methacrylate onto natural fibres and its effect on the mechanical properties of composites. *Journal of Applied Polymer Science, 131*(3), 398–406. [Crossref]

Abdulkadir, S. A., Muktari, S., Zakari, Y. I., Okpanachi, C. B., Mohammed, I. A., Yusuf, O. L., & Ojobo, L. O. (2025). The effect of ground rubber tire (GRT) filler particle size on the morphological, thermal and mechanical properties of waste high-density polyethylene (rHDPE). *UMYU Scientifica, 4*(3), 223–231. [Crossref]

Abu Bakar, A., Nik Mat, N. S., & Kamaruddin Isnin, M. (2008). Optimized conditions for the grafting reaction of poly(methyl methacrylate) onto oil-palm empty fruit bunch fibers. *Journal of Applied Polymer Science, 110*(2), 847–855. [Crossref]

Akil, H. M., Omar, M. F., Mazuki, A. A. M., Safiee, S., Ishak, Z. A. M., & Abu Bakar, A. (2011). Kenaf fiber reinforced composites: A review. *Materials & Design*, 32(8–9), 4107–4121. [Crossref]

Athawale, V. D., & Kolekar, S. L. (2000). Graft copolymerization of methyl acrylate onto starch using ceric ammonium nitrate as an initiator in aqueous medium. *European Polymer Journal, 36*(9), 1919–1926. [Crossref]

Bledzki, A. K., & Gassan, J. (1999). Composites reinforced with cellulose-based fibres. *Progress in Polymer Science*, 24(2), 221–274. [Crossref]

Danladi, E., Mamza, P. A. P., Yaro, S. A., Isa, M. T., Sadiku, R. E., & Ray, S. S. (2025). Reinforcing effect of jute fibre on the mechanical, dynamic mechanical and physical properties of polypropylene. *UMYU Scientifica, 4*(2), 25–31. [Crossref]

Faruk, O., Bledzki, A. K., Fink, H. P., & Sain, M. (2012). Biocomposites reinforced with natural fibers: 2000–2010. *Progress in Polymer Science*, 37(11), 1552–1596. [Crossref]

George, J., Sreekala, M. S., & Thomas, S. (2016). A review on interface modification and characterization of

natural fibre reinforced plastic composites. *Polymer Engineering & Science, 56*(5), 451–472. [Crossref]

Gupta, M. K., Srivastava, R. K., & Tripathi, R. K. (2013). Effect of surface modification on thermal and mechanical properties of natural fibre composites. *Composites Part B: Engineering, 45*(1), 601–607. [Crossref]

Huda, M. S., Drzal, L. T., Misra, M., & Mohanty, A. K. (2006). Chopped glass and recycled newspaper as reinforcement fibers in injection molded poly(lactic acid) (PLA) composites: A comparative study. *Composites Science and Technology, 66*(11–12), 1813–1824. [Crossref]

Jawaid, M., & Abdul Khalil, H. P. S. (2011). Cellulosic/synthetic fibre reinforced polymer hybrid composites: A review. *Carbohydrate Polymers*, 86(1), 1–18. [Crossref]

Jibril, A., Ishiaku, U. S., Musa, M. B., Giwa, A., & Ali, S. M. (2025). Development of epoxy-based particulate composite cladding from *Prosopis africana* pods. *UMYU Scientifica, 4*(3), 83–90. [Crossref]

John, M. J., & Thomas, S. (2008). Biofibres and biocomposites. *Carbohydrate Polymers, 71*(3), 343–364. [Crossref]

John, M. J., & Thomas, S. (2008). Biofibres and biocomposites. *Carbohydrate Polymers*, 71(3), 343–364. [Crossref]

Jonoobi, M., Harun, J., Mathew, A. P., Oksman, K., & Davoodi, N. H. (2011). Characteristics of kenaf (*Hibiscus cannabinus*) fibre and its composites: A review. *Carbohydrate Polymers, 83*(3), 1445–1455. [Crossref]

Kabir, M. M., Wang, H., Lau, K. T., & Cardona, F. (2012). Chemical treatments on plant-based natural fibre reinforced polymer composites: An overview. *Composites Part B: Engineering*, 43(7), 2883–2892. [Crossref]

Kalia, S., Kaith, B. S., & Kaur, I. (2009). Pretreatments of natural fibers and their application as reinforcing material in polymer composites: A review. *Polymer Engineering & Science, 49*(7), 1253–1272. [Crossref]

Kalia, S., Kaith, B. S., & Kaur, I. (2011). Pretreatments of natural fibers and their application as reinforcing material in polymer composites—A review. *Polymer Engineering & Science*, 49(7), 1253–1272. [Crossref]

Khalil, H. A., Bhat, A. H., & Jawaid, M. (2010). Cell wall ultrastructure, anatomy, lignin distribution, and chemical composition of Malaysian cultivated kenaf fibre. *Industrial Crops and Products, 31*(1), 113–121. [Crossref]

Li, X., Tabil, L. G., & Panigrahi, S. (2007). Chemical treatments of natural fibre for use in natural fibre-reinforced composites: A review. *Journal of Polymers and the Environment, 15*(1), 25–33. [Crossref]

Mwaikambo, L. Y., & Ansell, M. P. (2002). Chemical modification of hemp, sisal, jute, and kapok fibres by alkalization. *Journal of Applied Polymer Science, 84*(12), 2222–2234. [Crossref]

Panthapulakkal, S., & Sain, M. (2007). Injection-molded short hemp fiber/glass fiber-reinforced polypropylene hybrid composites: Mechanical, water absorption and thermal properties. *Journal of Applied Polymer Science, 103*(4), 2432–2441. [Crossref]

Pickering, K. L., Efendy, M. G. A., & Le, T. M. (2016). A review of recent developments in natural fibre composites and their mechanical performance. *Composites Part A: Applied Science and Manufacturing*, 83, 98–112. [Crossref]

Poletto, M., Zattera, A. J., Forte, M. M. C., & Santana, R. M. C. (2012). Thermal decomposition of wood: Influence of wood components and cellulose crystallite size. *Bioresource Technology, 109*, 148–153. [Crossref]

Sánchez-Silva, L., López-González, D., Villaseñor, J., Sánchez, P., & Valverde, J. L. (2012). Thermogravimetric-mass spectrometric analysis of lignocellulosic and marine biomass pyrolysis. *Bioresource Technology, 109*, 163–172. [Crossref]

Sanjay, M. R., Siengchin, S., Parameswaranpillai, J., & Jawaid, M. (2018). Natural fibre reinforced polymer composites: Characterization and applications. *Materials Today: Proceedings, 5*(1), 1785–1790. [Crossref]

Sinha, E., & Rout, S. K. (2008). Influence of fibre surface treatment on structural, thermal, and mechanical properties of jute fibre and its composites. *Bulletin of Materials Science, 31*(7), 791–799. [Crossref]

Tee, T. T., Sanyang, M. L., Ishak, N. S., & Abu Bakar, N. (2013). Fourier transform infrared (FTIR) spectroscopic analysis of modified natural fibre reinforced polymer composites. *Polymer-Plastics Technology and Engineering, 52*(12), 1234–1242. [Crossref]

Thakur, V. K., & Thakur, M. K. (2014). Processing and characterization of natural cellulose fibers/thermoset polymer composites. *Carbohydrate Polymers*, 109, 102–117. [Crossref]

Thakur, V. K., Thakur, M. K., & Gupta, R. K. (2014a). Graft copolymers of natural fibers for green composites. *Carbohydrate Polymers, 104*, 87–93. [Crossref]

Tomaz de Souza, T., Pereira, M. P. R., Leite, M. F., Pinto, P. H. P. M. de S., Paskowski, A. P., & Nunes, L. F. C. (2021). Thermal and chemical characterization of kenaf fibre (*Hibiscus cannabinus*) reinforced epoxy matrix composites. *Polymers, 13*(12), 2016. [Crossref]

Tserki, V., Zafeiropoulos, N. E., Simon, F., & Panayiotou, C. (2005). A study of the effect of acetylation and propionylation surface treatments on natural fibres. *Composites Part A: Applied Science and Manufacturing, 36*(8), 1110–1118. [Crossref]

Xie, Y., Hill, C. A. S., Xiao, Z., Militz, H., & Mai, C. (2010). Silane coupling agents used for natural fiber/polymer composites: A review. *Composites*

Part A: Applied Science and Manufacturing, 41(7), 806–819. [Crossref]

Yang, H., Yan, R., Chen, H., Lee, D. H., & Zheng, C. (2006). Characteristics of hemicellulose, cellulose, and lignin pyrolysis. *Fuel, 86*(12–13), 1781–1788. [Crossref]

Yang, H., Yan, R., Chen, H., Zheng, C., Lee, D. H., & Liang, D. T. (2007). Mechanism of palm oil waste pyrolysis in a fixed-bed reactor. *Energy & Fuels, 21*(2), 983–991. [Crossref]